

VIP21-Caveolin, a Membrane Protein Constituent of the Caveolar Coat, Oligomerizes In Vivo and In Vitro

Solange Monier,* Robert G. Parton,[†] Frank Vogel,* Joachim Behlke,*
Annemarie Henske,* and Teymuraz V. Kurzchalia*[†]

*Department of Cell Biology, Max-Delbrück Centre for Molecular Medicine, 13 122 Berlin-Buch, Germany; [†]Cell Biology Programme, European Molecular Biology Laboratory, Postfach 10.2209, 69012 Heidelberg, Federal Republic of Germany

Submitted January 25, 1995; Accepted May 3, 1995
Monitoring Editor: Guido Guidotti

VIP21-caveolin is a membrane protein, proposed to be a component of the striated coat covering the cytoplasmic surface of caveolae. To investigate the biochemical composition of the caveolar coat, we used our previous observation that VIP21-caveolin is present in large complexes and insoluble in the detergents CHAPS or Triton X-114. The mild treatment of these insoluble structures with sodium dodecyl sulfate leads to the detection of high molecular mass complexes of approximately 200, 400, and 600 kDa. The 400-kDa complex purified to homogeneity from dog lung is shown to consist exclusive of the two isoforms of VIP21-caveolin. Pulse-chase experiments indicate that the oligomers form early after the protein is synthesized in the endoplasmic reticulum (ER). VIP21-caveolin does indeed insert into the ER membrane through the classical translocation machinery. Its hydrophobic domain adopts an unusual loop configuration exposing the N- and C-flanking regions to the cytoplasm. Similar high molecular mass complexes can be produced from the in vitro-synthesized VIP21-caveolin. The complex formation occurs only if VIP21-caveolin isoforms are properly inserted into the membrane; formation is cytosol-dependent and does not involve a vesicle fusion step. We propose that high molecular mass oligomers of VIP21-caveolin represent the basic units forming the caveolar coat. They are formed in the ER and later, between the ER and the plasma membrane, these oligomers could associate into larger detergent-insoluble structures.

INTRODUCTION

Caveolae or plasmalemmal vesicles are nonclathrin-coated membrane invaginations that are found on the plasma membrane of almost all types of cells (for reviews see Anderson, 1993a; Anderson *et al.*, 1992; and references therein). Using various electron microscopic techniques, it has been possible to visualize the fine caveolar structure (Montesano *et al.*, 1982; Peters *et al.*, 1985; Anderson, 1991; Steer and Heuser, 1991; Rothberg *et al.*, 1992). On the cytoplasmic surface, multiple filaments can be seen wrapped around the invaginated plasma membrane. When viewed en face these filaments appear as a striated coat.

The function of caveolae is still uncertain although several possibilities have been postulated, including an alternative pathway of endocytosis (Montesano *et al.*, 1982; Simionescu *et al.*, 1982; Tran *et al.*, 1987); transcytosis (Ghitescu *et al.*, 1986); receptor-mediated uptake of small molecules (potocytosis; Rothberg *et al.*, 1990; Anderson *et al.*, 1992); intracellular calcium concentration regulation (Fujimoto, 1993; Fujimoto *et al.*, 1993); and signal transduction (Anderson, 1993b; Sargiacomo *et al.*, 1993; Lisanti *et al.*, 1994a).

The investigation of caveolae was greatly enhanced by the identification of a caveolar protein marker. Antibodies against a protein of 22 kDa, which was initially identified as one of the main substrates of src kinase in *v-src*-transformed cells (Glenney, 1989; Glenney and Zokas, 1989), decorated the caveolar filaments (Rothberg *et al.*, 1992). The protein was termed

[†] Corresponding author.

caveolin and was suggested to be a component of the coat material (Rothberg *et al.*, 1992). The chicken caveolin is almost identical to canine VIP21 (vesicular integral membrane protein of 21 kDa) (Glenney, 1992; Glenney and Soppet, 1992). The latter protein was identified through research on protein sorting in polarized epithelial cells as a constituent of *trans*-Golgi-derived vesicles (Kurzchalia *et al.*, 1992). VIP21-caveolin is an integral membrane protein: it cannot be extracted from membranes by either high salt or carbonate treatment (Dupree *et al.*, 1993). Subsequently, VIP21 was also localized to caveolae and the *trans*-Golgi-network (TGN)¹ (Dupree *et al.*, 1993).

Apart from the localization of VIP21-caveolin to caveolae, very little is known about the coat constituents (e.g. interaction partners of VIP21-caveolin) or the mechanisms governing the formation of caveolar filaments. In this respect, the fact that VIP21-caveolin is not solubilized by detergents such as 3-[(3-cholamidopropyl)-dimethylammonio]-1-propane sulfonate (CHAPS) or Triton X-100 could be a useful tool. VIP21-caveolin was one of the proteins found in detergent-insoluble structures together with an apically destined integral membrane protein, influenza hemagglutinin (HA), after treatment of TGN-derived vesicles isolated from Madin-Darby canine kidney (MDCK) cells with detergents (Kurzchalia *et al.*, 1992). Also, glycosylphosphatidyl-inositol (GPI)-anchored proteins, which according to morphological studies concentrate in caveolae (Rothberg *et al.*, 1990), were found in a Triton-insoluble floating fraction (later referred to as TIFF) (Hoessli and Rungger-Brändle, 1985; Brown and Rose, 1992). TIFF, like caveolae, is enriched in cholesterol and glycosphingolipids (Montesano *et al.*, 1982; Rothberg *et al.*, 1990; Brown and Rose, 1992; Fiedler *et al.*, 1993; Parton, 1994). All together, these data led to the hypothesis that TIFF is similar, if not identical, to caveolae (Lisanti *et al.*, 1993; Sargiacomo *et al.*, 1993). Recently, some of these proteins have been identified (Arreaza *et al.*, 1994; Chang *et al.*, 1994; Fiedler *et al.*, 1994; Lisanti *et al.*, 1994b). These proteins, including the src kinases, rab proteins, the thrombospondin receptor (CD36), gelsolin, and even albumin, have very different structures and a wide range of functions. It is likely that the detergent-insoluble material is derived from various intracellular membranes, including the TGN and caveolar membrane domains. Because of their biochemical nature, some proteins become included in this material but obviously have nothing to

¹ Abbreviations used: 2D, two dimensional; DPM, dog pancreas microsomes; ER, endoplasmic reticulum; GH, growth hormone; GPI, glycosylphosphatidyl-inositol; GS, glycosylation site; SRP, signal recognition particle; TGN, *trans*-Golgi network; TIFF, Triton-insoluble floating fraction; TR VIP, truncated form of VIP21-caveolin, deleted of its first 31 amino acids; WT VIP, wild-type VIP21-caveolin.

do with caveolae. Therefore, the localization of each protein identified in the detergent-insoluble material and its interaction with VIP21-caveolin must be investigated carefully.

The study of biochemical properties of VIP21-caveolin is very important in terms of vesicular transport. There must be fundamental differences between formation of clathrin or COP-containing vesicular coats on the one hand and the caveolar coat on the other. The first two consist almost entirely of soluble proteins whereas VIP21-caveolin is an integral membrane protein. Obviously, the cellular location of the VIP21-caveolin insertion into the membrane and its membrane topology should directly influence interaction of VIP21-caveolin with other caveolar proteins and the formation of the caveolar filaments. For instance, the topology of VIP21-caveolin could have an implication on its interaction with GPI-anchored proteins. There is still controversy concerning whether both N- and C-domains of VIP21-caveolin are facing the cytoplasm (Dupree *et al.*, 1993), or if VIP21-caveolin is a type II membrane protein with its C-terminus exposed to the outside of the cell (Sargiacomo *et al.*, 1993). A direct interaction between VIP21-caveolin and the polypeptide chain of a GPI-anchored protein would occur only if the second orientation is correct.

To address some of the problems mentioned above, we have studied the biosynthetic pathway of VIP21-caveolin, its membrane topology, and properties of the VIP21-caveolin-containing complexes in detail.

MATERIALS AND METHODS

Materials

Detergents were purchased from Calbiochem (San Diego, CA). Reagents for SDS-polyacrylamide gel electrophoresis (PAGE) were obtained from ICN (Meckenheim, Germany). Nitrocellulose filter-paper was obtained from Schleicher & Schuell (Dassel, Germany); protein-A sepharose was obtained from Pharmacia (Upsala, Sweden) or from Sigma (Deisenhofen, Germany). The chemiluminescence-detection kit (ECL) and [³⁵S]methionine were obtained from Amersham (Buckinghamshire, UK); proteinase K, chymotrypsin, and endoglycosidase F were obtained from Boehringer (Mannheim, Germany). Trypsin was obtained from Promega (Heidelberg, Germany). The protein marker kit for very high molecular weights, brefeldin A, aprotinin, and phenylmethylsulfonyl fluoride (PMSF) were obtained from Sigma (Deisenhofen, Germany). The cell culture medium, reagents, and Geneticin (G418) were obtained from Life Technologies (Eggenstein, Germany); the cell culture dishes were obtained from Nunc (Roskilde, Denmark). The reagents used for cDNA cloning, for in vitro transcription, translation, and translocation were obtained from the sources described in Monier *et al.* (1988). The rabbit polyclonal antibody directed against the N-region (amino acids 14–33) (VIP21-N) was a gift from Dr. Paul Dupree (University of Cambridge, UK). HeLa cells were a gift from Dr. Bill Dolan (New York University Medical Center, New York, NY).

Preparation of CHAPS Complex from Total Cell Membrane Fraction

For analytical purposes, the CHAPS complex was prepared from MDCK cells as previously described (Kurzchalia *et al.*, 1992; Fiedler

et al., 1993) with the following modification. Instead of a flotation gradient, the post nuclear supernatant was centrifuged at $100,000 \times g$ for 1 h. The resulting microsomal pellet was treated with 20 mM CHAPS at 4°C and spun on a 10–30% linear sucrose gradient in a SW40 rotor at 38,000 rpm for 2.5 h. The pellet was solubilized with SDS-PAGE sample buffer and subjected to electrophoresis.

Preparation of TIFF from MDCK Cells and Dog Lung

TIFF from dog lung was prepared according to a modified procedure described for MDCK cells (Fiedler *et al.*, 1993). Forty grams of canine lung were minced and homogenized with a Potter-homogenizer in Hoagland buffer (50 mM Tris/HCl, pH 7.5, 25 mM KCl, 5 mM $MgCl_2$, 0.2 mM EDTA, 250 mM sucrose, and 0.2 mM PMSF, added fresh before homogenization). The ratio of tissue to buffer was 1:2.5 and seven strokes at maximal rotation rate were applied. The homogenate was centrifuged for 20 min at $10,000 \times g$ and filtered through a cloth. After 75 min of centrifugation at 28,000 rpm in a Ti35 rotor, the microsomal pellet was resuspended in 7.5 ml of 250 mM sucrose in TNE (25 mM Tris/HCl, pH 7.5, 100 mM NaCl, 2 mM EDTA) containing 5 mM β -mercaptoethanol, and brought to 1.5 M sucrose in a total volume of 10 ml. The solution was overlaid by 17 ml of 1.2 M sucrose and 7 ml of 0.8 M sucrose, both sucrose solutions containing TNE and 5 mM dithiothreitol (DTT). After centrifugation in an SW28 rotor for 20 h at 28,000 rpm, the total membrane fraction was collected at the 0.8/1.2 M sucrose interface.

This fraction was extracted with 1% Triton X-114 in TNE and protease inhibitors in a total volume of 10 ml. The extract was brought to 1.4 M sucrose, a 4-ml fraction was overlaid by 6 ml and 2 ml of 1.1 M and 0.15 M sucrose, respectively. Flotation was carried out for 21 h at 39,000 rpm in a SW40 rotor. The opalescent interface between 1.1 M and 0.15 M sucrose was collected (7.5 ml), diluted to 36 ml with TNE, and centrifuged in SW40 for 8 h at 39,000 rpm. The pellets were resuspended in 1% Triton X-114 in TNE, incubated on ice for 30 min, and brought to 1.4 M sucrose. The previous flotation procedure was repeated and the resulting pellets were resuspended in 18 ml of 1% Triton X-114 in TNE (TIFF).

The TIFF was heated to 37°C under permanent vortexing. After 15 min, the suspension was chilled on ice for 5 min and centrifuged for 15 min at $10,000 \times g$. The resulting pellet was used for high molecular mass complex isolation.

Isolation of the 400-kDa Complex

The pellet (P) was resuspended in 1 ml of alkaline SDS-PAGE sample buffer lacking bromophenol blue. For analytical purposes, 100 ml aliquots were incubated at 25°C and overlaid onto a 4 ml 10–30% linear sucrose gradient containing 0.2% SDS and TNE. The gradients were centrifuged in a SW60 rotor at 40,000 rpm for 19 h at 19°C. Aliquots of the recovered 0.5-ml fractions were mixed with alkaline sample buffer, incubated at 25°C, or boiled and processed for Western blot analysis using the VIP21-N antibody.

Preparative isolation of the 400-kDa complex was performed from 0.8 ml of the P fraction treated by 1% SDS at room temperature and overlaid onto an 11-ml 10–30% continuous sucrose gradient. After a 23-h centrifugation at 39,000 rpm in a SW40 rotor, 1-ml fractions were collected, and the amount of VIP21-caveolin present in each fraction was analyzed by Western blot analysis. The peak fraction (1 ml) was dialyzed against TNE containing 0.2% SDS and subjected to an identical sucrose gradient centrifugation.

Determination of an S-Value of the 400-kDa Complex

After velocity sucrose gradient centrifugation, the peak fraction containing purified VIP21-caveolin was dialyzed against 2×200 ml of buffer containing 50 mM Tris-HCl, pH 7.5, 0.2% SDS, and 50 mM

DTT. The S-value at 20°C was determined using an UV-detection system with photoelectric scanner (Behlke *et al.*, 1986).

Electron Microscopy

Samples of TIFF or gradient fractions were incubated on formvar-coated grids, rinsed with detergent-free TN buffer (25 mM Tris-HCl, pH 7.5, 100 mM NaCl), and then negatively stained with uranyl acetate. For immunolabeling, grids were incubated sequentially with affinity-purified VIP21-N antibodies and 5 nm protein A-gold in TN buffer before negative staining. Antibodies and washing solutions were centrifuged at maximum speed in the microfuge for 5 min or filtered before use. An irrelevant antibody (affinity-purified rabbit anti-rab2, kindly provided by Dr. Marino Zerial, EMBL, Heidelberg), used at the same concentration as the VIP21-N, gave no significant labeling.

SDS-PAGE and Blotting Techniques

Most techniques were performed as previously described (Kurzchalia *et al.*, 1992). Two SDS-PAGE sample buffers were used: the standard buffer, containing 12.5 mM Tris-HCl, pH 6.8, and the alkaline buffer, containing 12.5 mM Tris-base (the other components being the same for both: 2% SDS, 1% β -mercaptoethanol, 0.00125% bromophenol blue, and 10% glycerol). High molecular mass complexes were separated on 2.5–7.5% or 2.5–16% acrylamide gradient gels with a 2.5% or 3% stacking gel. The samples in the standard or in the alkaline sample buffer were incubated at 25°C for 30 min or boiled for 5 min as indicated in the legends to figures. When 2D gel analysis was carried out, the first dimension involved the separation of large complexes present in nonboiled samples on a 2.5–7.5% resolving gel. Each lane was cut, boiled in a bag containing alkaline sample buffer, and loaded on the second dimension, 3–16% resolving gel.

Cell Culture, Transfection, Radioactive Labeling, and Immunoprecipitation Techniques

MDCK cells were grown as described in Kurzchalia *et al.* (1992). HeLa cells were maintained and transfected according to Monier *et al.* (1988), except that the *in vivo* expression vector pSV2 TKneo was used (Compton *et al.*, 1989). Permanent transformants were selected by their growth in the G418-containing medium. Individual clones were screened for overexpression of the wild-type VIP21 by immunoprecipitation: after overnight metabolic labeling in the presence of 80 mCi/ml of [35 S]methionine and 5 mM sodium butyrate (Monier *et al.*, 1988), the cells were solubilized in a lysis buffer (Dupree *et al.*, 1993) and the whole extract was incubated for 20 h with the VIP21-N antibody.

Pulse-chase experiments were performed on subconfluent cultures grown in 35-mm dishes. After an induction with 5 mM sodium butyrate for 6.5 h, cells were incubated in serum-free, methionine-free medium for 30 min, then pulse-labeled in fresh medium supplemented with 150 mCi/ml of radioactive methionine for 7 min, and chased in medium containing 10% fetal calf serum and a 30-fold excess of cold methionine for various time points. Cells were solubilized and immunoprecipitated as described above.

The brefeldin A treatment was performed according to Ivessa *et al.* (1992), except that the cells were given a 10-min pulse of radioactive methionine and further incubated in the chase medium for 1 h or 4 h before solubilization and immunoprecipitation.

Cloning Procedures

Fusion proteins containing a glycosylation site placed upstream from the portion of rat growth hormone (GH) comprised between amino acids 42 and 130, and various parts of VIP21, were constructed using the polymerase chain reaction (PCR) technique. First, preGH was deleted of its signal peptide (amino acids 1–26) and of

the next 15 residues (which present a relatively high hydrophobicity and could potentially act as a signal peptide). A glycosylation site was added at position 2 (Met Asn Gly Thr), the same site as the one present in the opsin protein (see Monier *et al.*, 1988). The reaction was performed using the wild-type GH as a template, a sense 50 mer hybridizing to the 5' end of the insert and containing the cloning site *SacI*, the glycosylation site including a *BamHI* site and a region encoding the amino acids 42–50 of GH, and a primer complementary to the vector sequence at the 3' end. The PCR product was cloned in the *SacI/PstI* of pSP65 to generate pGSΔGH. Second, the PCR was performed using VIP21 cloned in the Bluescript vector as a template (Kurzchalia *et al.*, 1992) and primers at the 5' end generating a *KpnI* site either at the N-terminus of VIP21 (before amino acid 1), or just before the hydrophobic sequence and the C-tail (before amino acid 101), or before the C-tail only (before amino acid 135); the same primer complementary to the vector sequence was used for the 3' end in the three reactions. The three PCR products were digested with *KpnI* and *PstI*, and cloned in pGSΔGH cut with the same enzymes. The resulting constructs GSΔGH-FL VIP, -HSC VIP, and -C VIP are fusion proteins consisting of a glycosylation site linked to the segment of GH comprised between residues 42 and 130, and either the full length VIP21, or the hydrophobic sequence plus the C-tail (amino acids 102–178), or the C tail of VIP (amino acids 135–178), respectively.

Two glycosylation sites were added to the wild-type VIP21, one at the N-terminus of the protein and identical to the one just described, the other added at the C-terminus, located at position 179, just after the last codon of the native protein. This construct was made by PCR, using VIP21 in pSP65 as a template, a 22 mer sense oligonucleotide coding for amino acids 2–6 of the native VIP21 and having a *BamHI* site at its 5' end, a 28 mer antisense primer coding for the last 6 amino acids of VIP21 and for a glycosylation site including a *KpnI* site. The PCR product was digested with *BamHI* and *KpnI*, and cloned in the GSΔGH-C VIP. The resulting clone GSVIPGS encodes a modified VIP21 with three extra residues at the N-terminus (Asn Gly Thr) located before amino acid 2 of the native VIP21, and with Asn Gly Ser located after the last residue of the native VIP21 and followed by the duplicate of the C-tail of the protein (43 amino acids).

The truncated form of VIP21 (TR VIP) was obtained by cloning the *NcoI-KpnI* fragment of VIP21 in a plasmid providing the new initiation codon, pSP450 (Monier *et al.*, 1988) and cut with *NcoI* and *KpnI*. The resulting TR VIP clone encodes the VIP21-caveolin protein deleted of its first 31 amino acids.

The modifications introduced in the various plasmids were confirmed by DNA sequencing.

***In Vitro* Transcription, Translation, Translocation, and Post-translational Assays**

All of the cDNAs used for *in vitro* transcription were cloned in vectors pSP64 or pSP65, under the control of the SP6 promoter. *In vitro* transcription, translation in the wheat germ system, and translocation across dog pancreas microsomes were carried out as previously described (Monier *et al.*, 1988). Puromycin-high potassium-washed rough microsomes (PKRM), SRP, and reconstituted proteoliposomes (Görlich and Rapoport, 1993) were generous gifts of Berit Jungnickel and Tom Rapoport (MDC, Berlin-Buch, Germany).

The flotation assay was performed either under high salt or under alkaline pH conditions as follows: 10 μ l of translation mix was adjusted to 0.6 M NaCl and 20 mM EDTA (high salt flotation) or to 0.24 M Na₂CO₃, pH 13, and 2 M sucrose (alkaline pH), and both were incubated on ice for 30 min. A 2.1 M sucrose (final concentration) was added to the latter sample, mixed well, and 0.6 ml of both samples were overlaid by 0.8 ml of 1.3 M sucrose and 0.8 ml of 0.5 M sucrose, all the sucrose solutions being adjusted to the same salt concentration or to the same pH as the sample being processed. After a 2.5-h centrifugation at 50,000 rpm in a SW60 rotor, the

floated membranes were recovered at the 0.5 M/1.3 M interface; the fraction that remained in the 2 or 2.1 M sucrose represents the free fraction, i.e., nonmembrane associated. Both fractions were precipitated with trichloroacetic acid and analyzed by SDS-PAGE.

The protease protection assay was performed by incubating on ice the *in vitro*-translated samples in the presence of 0.7 mg/ml proteinase K for 1 h or in the presence of a mixture of trypsin and chymotrypsin at 0.14 mg/ml each for 80 min. PMSF (10 mM) or 1000 U/ml aprotinin was added to inactivate the proteinase K and the trypsin/chymotrypsin, respectively, before solubilizing the reaction mix in the usual SDS-PAGE sample buffer. The endoglycosidase F treatment was carried out as follows: translation products were denatured by boiling in the presence of 0.5% SDS and 1% β -mercaptoethanol; 1.25% NP40 was then added and samples were incubated without (mock treatment) or with 5 U/ml endoglycosidase F for 1 h 40 min at 37°C. The reaction was stopped by adding the gel sample buffer and boiling.

The post-translational assay used for generating VIP21-caveolin oligomers *in vitro* was performed according to the following procedure: after usual protein synthesis, 4 μ l translation mix were incubated for 90 min at 30°C in the presence of cytosol (a 100,000 \times g supernatant of HeLa or MDCK cells, homogenized using a ball-bearing homogenizer in 50 mM *N*-2-hydroxyethylpiperazine-*N'*-2-ethanesulfonic acid (HEPES), pH 7.2, 1 mM Mg(OAc)₂, 90 mM KOAc, 0.5 mM DTT, 1 mM ATP) in a total volume of 6–8 μ l. In some experiments, to keep the reaction volume small enough so that it could be loaded on the gel without further treatment, the translation mix was centrifuged at 12,000 rpm for 4 min before the post-translational assay, the supernatant was discarded, and the pellet was resuspended in a buffer (HMKD) containing the same ion concentration as the translation mix: 20 mM HEPES, pH 7.6, 1 mM Mg(OAc)₂, 60 mM KOAc, 0.2 mM DTT; this centrifugation step had no influence on the oligomerization process. The various cell extracts contained between 20 and 70 mg/ml protein, and were used at a final concentration of 5–12 mg/ml. The role of some potential components of the cytosol was tested by using various reagents added to the cytosol just before its addition to the translation mix: 10 mM EDTA, EGTA, or GMP-PCP, or 10 mM deoxyglucose plus 20 μ g/ml hexokinase were used for testing the role of Mg²⁺, Ca²⁺, GTP-, and ATP-hydrolysis, respectively, on the oligomerization process. The possible role of protease components of the cytosol was investigated by using a cytosol treated with the mixture trypsin/chymotrypsin at 0.14 mg/ml for 90 min on ice. The proteases were inactivated by 1000 U/ml of the protease inhibitor aprotinin, and this mixture was used in the post-translational assay as usual. The reaction products were analyzed by SDS-PAGE without boiling, unless otherwise indicated. Various processing was performed on the post-translational reaction mixture. The CHAPS extraction was performed according to Fiedler *et al.* (1993), except that smaller volume was used to avoid precipitating the sample with trichloroacetic acid; the trypsin/chymotrypsin digestion was performed the same way as for the protease protection assay of microsomes.

RESULTS

VIP21-Caveolin Is Extracted from Lung and Cultured MDCK Cells in the Form of High Molecular Mass Complexes Consisting of VIP21-Caveolin Monomers

Previous work has shown that, upon treatment of TGN-derived vesicles or of purified membrane fraction with the detergents CHAPS or Triton X-114 (Kurzchalia *et al.*, 1992; Fiedler *et al.*, 1993), VIP21-caveolin was found in large, insoluble structures. The protein was detected as a 21-kDa protein or a 21- to 20-kDa

doublet, after SDS-PAGE and immunoblotting using anti-N or an anti-C terminus antibodies, respectively (Dupree *et al.*, 1993). Our present work was aimed at characterizing components present in the VIP21-caveolin containing high molecular mass structures, and likely to be interaction partners of the protein in the cell.

A mild treatment of the CHAPS insoluble material isolated from MDCK cells with SDS was performed. The solubilization with SDS-PAGE sample buffer at 25°C resulted in the appearance of high molecular mass complexes, separated on a 2.5–7.5% acrylamide gel and detected by immunoblot using an antibody directed against the N-terminus of VIP21-caveolin (Figure 1, lanes 1 and 3). These complexes were not oxidized forms of VIP21-caveolin because the sample buffer contained 2% β -mercaptoethanol. Because estimation of the exact molecular masses of these complexes is difficult, we will refer to them as 200-, 400-, and 600-kDa complexes. They were disrupted partially upon boiling in the standard (pH 6.8) SDS-PAGE sample buffer (Figure 1, lane 2), or totally after boiling in alkaline sample buffer (Figure 1, lane 4). This gel did not allow the detection of the 21-kDa VIP21-caveolin monomer because proteins below 60 kDa migrated with the dye front.

The further analysis of the VIP21-caveolin-containing complexes was performed using TIFF from dog lung as a starting material (Fiedler *et al.*, 1993). Indeed, lung is one of the tissues in which VIP21-caveolin,

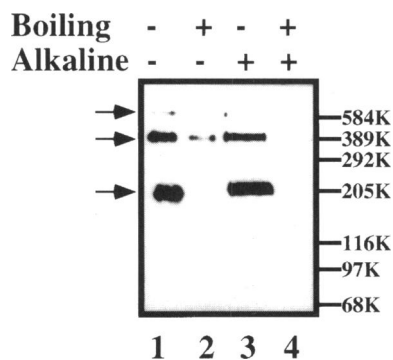


Figure 1. VIP21-caveolin is found in the form of high molecular mass complexes in MDCK cells. CHAPS-insoluble material from MDCK-cells was solubilized either in the standard SDS-PAGE sample buffer (lanes 1 and 2) or in the alkaline sample buffer (lanes 3 and 4) and incubated either at 25°C (lanes 1 and 3) or boiled for 5 min (lanes 2 and 4). The samples were analyzed on a 2.5–7.5% gel, which was blotted and subsequently incubated with VIP21-N antibodies. Arrows indicate high molecular mass complexes. Molecular mass markers here and in subsequent figures are: cross-linked hexamer of rabbit muscle phosphorylase b (584 K), tetramer of rabbit muscle phosphorylase b (389 K), trimer of rabbit muscle phosphorylase b (292 K), rabbit muscle myosin (205 K), β -galactosidase (116 K), rabbit muscle phosphorylase b (97 K), bovine serum albumin (68 K), chicken ovalbumin (45), bovine pancreas trypsinogen (24 K), and soybean trypsin inhibitor (20 K).

detected by immunoblot, is quite abundant (Glenney, 1992). A similar high molecular mass complex pattern was detected in CHAPS-pellet from MDCK cells and in TIFF from the lung. This pattern was also seen in a total membrane fraction not treated with detergent (our unpublished observation).

To purify the VIP21-caveolin-containing complexes from lung and characterize its composition, we used the fraction P from TIFF (see MATERIALS AND METHODS). The sample was solubilized in SDS at 25°C and submitted to a velocity sucrose gradient centrifugation. Fractions were collected, analyzed by SDS-PAGE after treatment at 25°C or at 95°C, and the VIP21-caveolin-containing complexes were detected by immunoblot using the VIP21-N antibody. The major species detected was the 400-kDa complex plus a minor 600-kDa band found in fractions 1 to 3 from the bottom of the tube (Figure 2A, lanes 1–3, arrow). After boiling (Figure 2B), the complexes were disrupted and generated the VIP21-caveolin of 21 kDa (Figure 2B, lanes 1–3, arrowheads). When the same SDS-solubilized starting material was boiled before centrifugation, VIP21-caveolin remained at the top of the gradient as a 21-kDa species (our unpublished observation). The silver staining of the same gels is shown in Figure 2, C and D, and clearly indicates that boiling of the 400-kDa species, essentially present in lanes 1–3 (Figure 2C, arrow), led to the appearance of the two 20- to 21-kDa VIP21-caveolin isoforms (Figure 2D, lanes 1–3, arrowheads). The complex was further purified by a second velocity gradient centrifugation. Within the detection limits of silver staining, it resolved exclusively into the VIP21-caveolin upon boiling (Figure 2E). The 400-kDa complex was subjected to analytical centrifugation for determination of its sedimentation properties. The obtained $S_{20,W}$ value of 14.4 together with the shape and size of the particle will allow more accurate estimation of the molecular mass of the complex (see below).

Electron Microscopy of TIFF and of Purified 400-kDa Complex

Examined morphologically, TIFF comprised heterogeneous membranous material. Large sheets of membrane, smaller vesicle-like structures, plus lamellae-like material were all observed (Figure 3A). This material was not labeled by VIP21-N antibodies but labeling was seen in patches on the membranous structures (our unpublished observation).

Different fractions of the SDS-treated lung TIFF separated by density gradient centrifugation were examined by negative staining. Fractions 1 and 2, which correspond to 400-kDa complexes (see Figure 2C), consisted of small groups of mainly ovoid structures (Figure 3, B–E). The majority of these

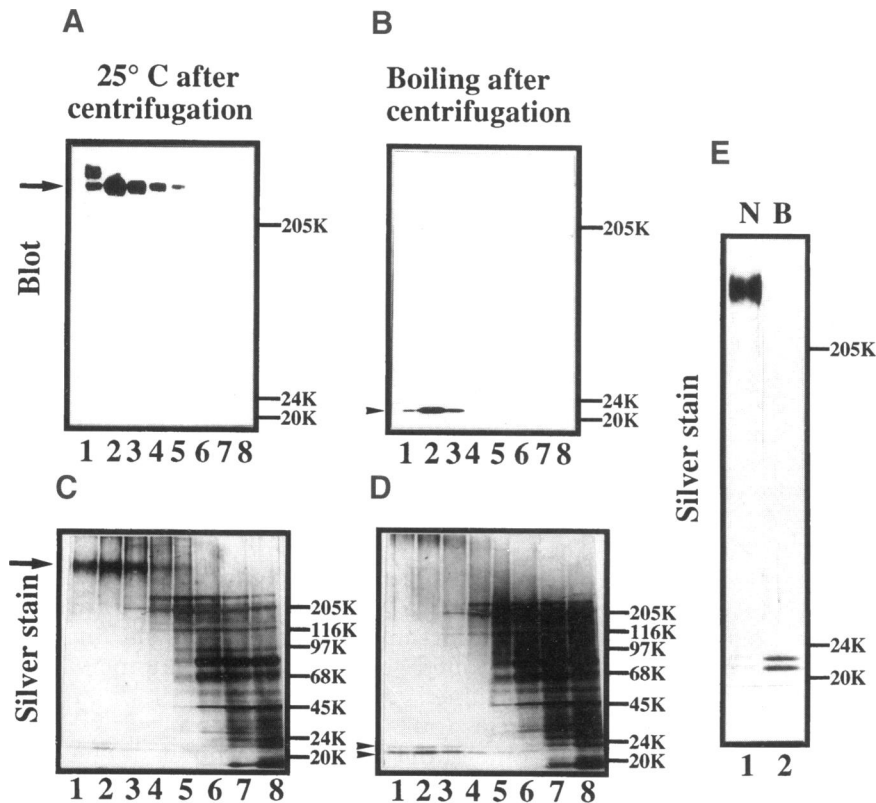


Figure 2. The high molecular mass complexes contain only VIP21-caveolin monomers. The P fraction from TIFF (see MATERIALS AND METHODS) was treated at 25°C before centrifugation on 10–30% sucrose gradients. Fractionation was performed from the bottom of the gradient and the numbers of the lanes correspond to the numbers of the gradient fraction. Aliquots of the fractions after centrifugation were treated at 25°C (panels A and C) or boiled (panels B and D). SDS-PAGE on a 2.5–15% gel, and either blotting to nitrocellulose and staining with VIP21-N antibodies (panels A and B), or silver staining (panels C and D) were performed. Panel E shows the silver staining of the purified 400-kDa complex treated at 25°C (N) or boiled (B). Arrow indicates high molecular mass complexes; arrowheads indicate VIP21-caveolin monomers.

structures were 15–17 nm long and 8–10 nm wide although larger particles were also occasionally observed. Most of these particles were present in groups. These structures were labeled by affinity-purified VIP21-N antibodies (Figure 3E). Fraction 5 contained large groups of ovoid structures as well as some thin filamentous material whereas fraction 8 contained lamellae-like material (similar to the VIP21-caveolin negative structures seen in the TIFF), which we assume represents lipid-rich complexes.

The estimation of the molecular mass of the 400-kDa complex was based on the dimensions and the shape of the particle and also on the amino acid composition of VIP21-caveolin. Taking into account different amounts of bound SDS, different molecular masses of the protein fraction in the complex were obtained (from 253 to 548 kDa for 50 and 100% of protein in the complex, respectively). This data together with the $S_{20,W}$ value were used to calculate the diffusion coefficient as well as the frictional ratio (f/f_0). The estimated value of the frictional ratio for the microscopically observed particle can be compared with values calculated for different SDS-protein complexes on the basis of hydrodynamic experiments. The best fit was observed at about 40% of bound SDS. We can speculate that the protein portion of the particle was about 310 kDa and would correspond to about 15 molecules

of VIP21-caveolin in the 400-kDa complex. The difference observed in molecular mass determined by SDS-PAGE can be explained by the fact that samples were not heat denatured. Also, the presence of lipids in the complex can further impair the molecular mass determination.

VIP21-Caveolin Is Found in High Molecular Mass Complexes Shortly After It Is Synthesized

As shown above, VIP21-caveolin was isolated at steady state in the form of high molecular mass complexes. Similar complexes were immunoprecipitated from a total MDCK cell extract, after an overnight metabolic labeling and subsequent immunoprecipitation with the VIP21-N antibody (Figure 4A). The cells were solubilized with a buffer containing 1% NP40, 0.4% sodium deoxycholate, and 0.4% SDS before immunoprecipitation. Upon boiling in the standard sample buffer, the high molecular mass complexes dissociated partially, generating exclusively the VIP21-caveolin monomers (Figure 4A, compare lanes 1 and 2) in about equimolar proportion. Some weak bands of approximately 45, 54, 100, and 220 kDa represented nonspecific background noise, which could not be competed with a large excess of N-peptide included in the

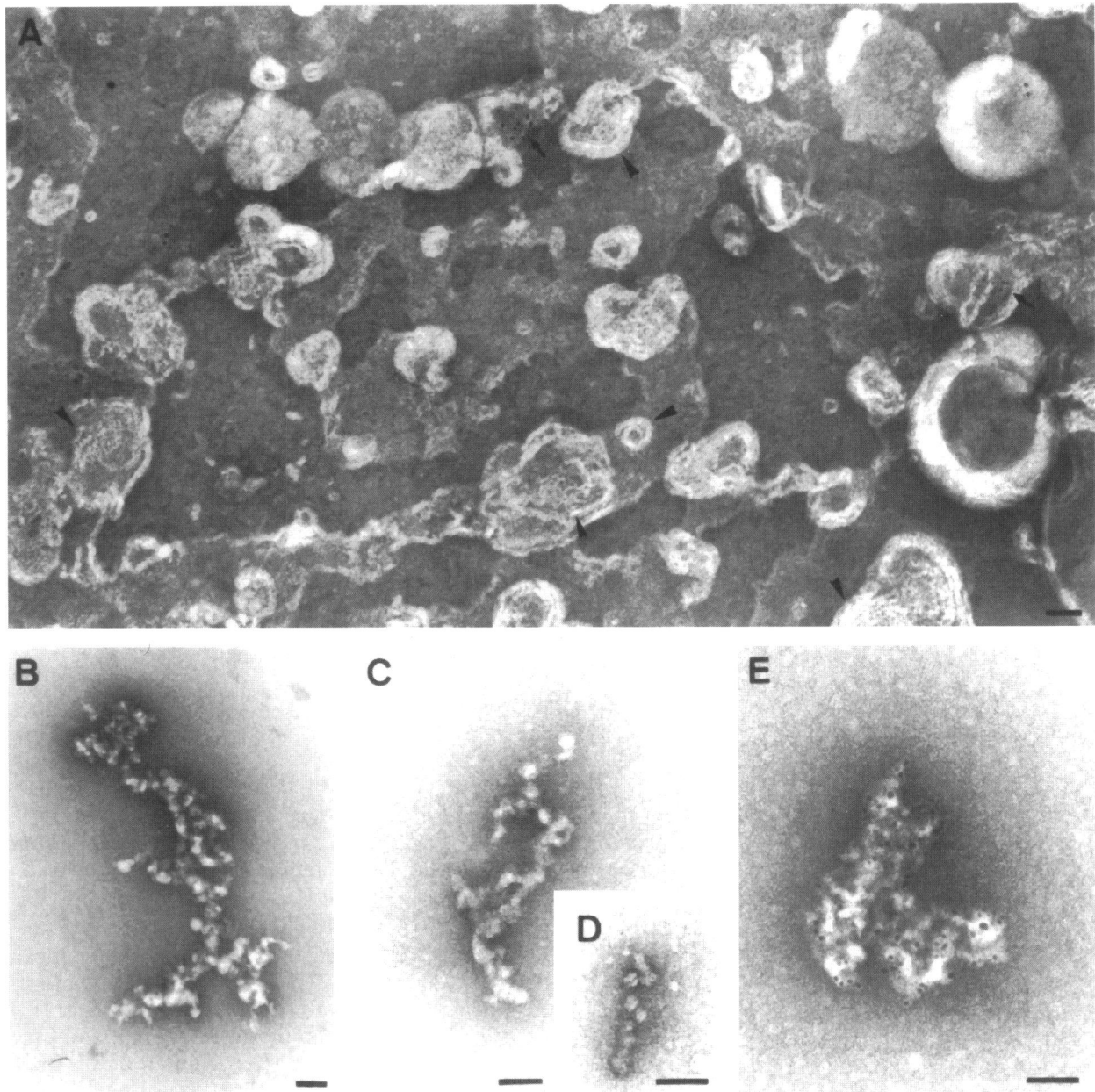
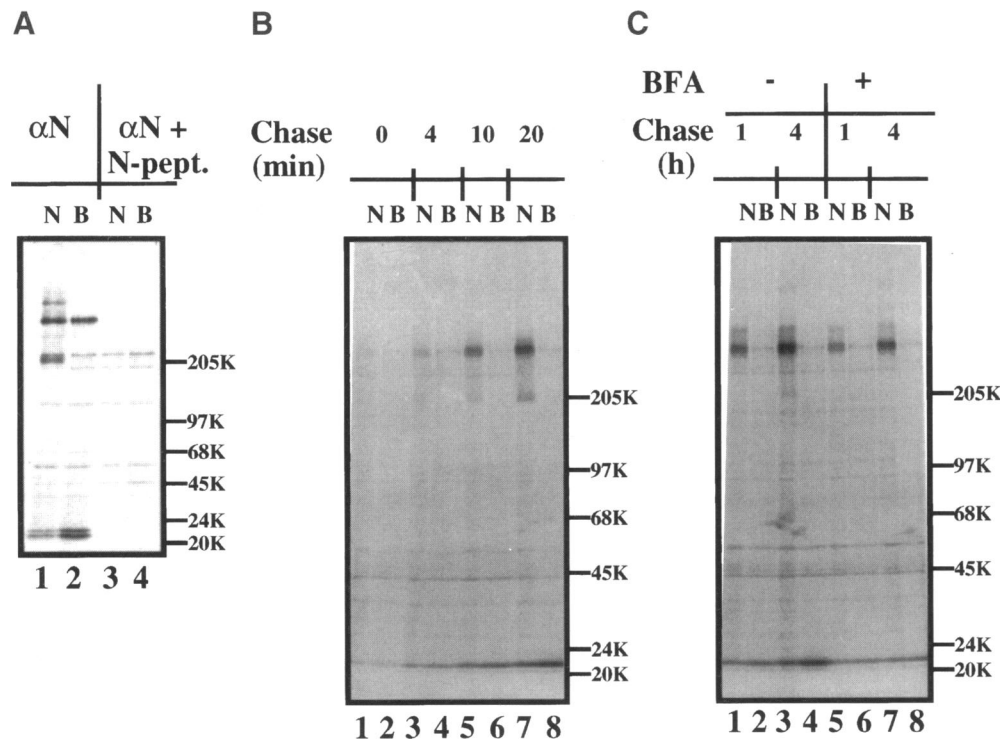


Figure 3. Morphological analysis of lung TIFF and purified 400-kDa complex. (A) TIFF was applied to a grid and immunolabeled using affinity-purified VIP-N antibodies before negative staining. Heterogeneous membranous structures, some of which are several microns in size, are apparent. Arrays of striated lamellae-like material, often arranged in concentric rings (see arrowheads), are abundant. Groups of VIP2-N gold particles are associated with various membrane fragments (e.g. see arrows) but rarely with the striated material. (B–E) TIFF was treated with SDS and was separated by sucrose density gradient centrifugation (see Figure 2). Fractions 1 and 2 were applied to grids and negatively stained. In panel E, the complexes were treated with antibodies to VIP21-caveolin before negative staining. The VIP21-caveolin complexes consist of ovoid structures usually clustered in groups which are labeled strongly with VIP21-N antibody (E). Note that in panel E, the structure of the individual ovoid structures is masked by the layer of antibody-protein A complexes. Bars: A, 500 nm; B–E, 50 nm.

immunoprecipitation assay (Figure 4A, compare lanes 3 and 4 to lanes 1 and 2).

A time-course study of the VIP21-caveolin complex appearance was performed on HeLa cells permanently transfected with VIP21-caveolin cDNA,

placed under the control of an inducible promoter, and thereby expressing a larger amount of VIP21-caveolin than the parent cell line or than the nontransfected MDCK cells. The majority of the VIP21-caveolin transfectants analyzed expressed



SDS-PAGE sample buffer. (C) VIP21-caveolin-transfected HeLa cells were incubated in methionine-free medium for 30 min, pulse-labeled for 10 min, and chased for 1 h or 4 h; 5 $\mu\text{g/ml}$ brefeldin A (BFA) was present during all these incubations. Immunoprecipitates were treated as indicated in panel B.

predominantly the larger isoform of the protein, and, as a possible consequence, the complexes immunoprecipitated by the VIP21-N antibody are of slightly different sizes (approximately 150, 300, and 400 kDa) than the ones identified in MDCK cells (Figure 4, panels B and C compared with panel A). After a 7-min pulse with radioactive methionine and no chase, a faint but definite band corresponding to the 300-kDa molecular mass complex could already be detected (Figure 4B, lane 1). The amount of complexes formed was more visible after a short chase period of 4 min or more (Figure 4B, from lane 3 on) and they resolved into the VIP21-caveolin monomer upon boiling in alkaline buffer.

Furthermore, brefeldin A, a drug that induces the redistribution of the Golgi to the ER (preventing the normal transport of proteins beyond the Golgi apparatus), did not seem to affect the formation of VIP21-caveolin oligomers, even if it was added 30 min before the 10-min pulse and was present during up to 4 h of chase (Figure 4C, lanes 1 and 3, compared with lanes 5 and 8). The results of these pulse-chase experiments strongly suggest that the complexes were formed early after the synthesis of the protein was completed and that no post-Golgi step is needed.

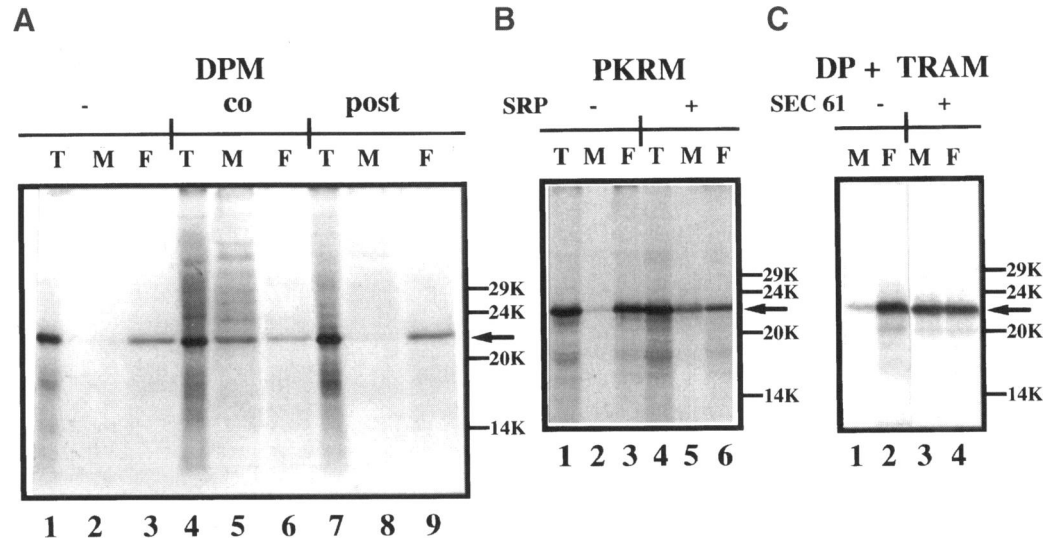
Figure 4. VIP21-caveolin is found in high molecular mass complexes early after its synthesis is completed; the complex formation is insensitive to brefeldin A treatment. (A) MDCK cells were metabolically labeled overnight with [^{35}S]methionine, the cells solubilized and immunoprecipitated with the VIP-N antibody, and the immunoprecipitate was solubilized in the standard SDS-PAGE sample buffer and treated at 25°C (N, odd number lanes) or boiled (B, even number lanes) before analysis by SDS-PAGE on a 2.5–16% acrylamide gradient gel and autoradiography. 25 $\mu\text{g/ml}$ N-peptide was added together with the VIP-N antibody as indicated (lanes 3 and 4). (B) HeLa cells permanently transfected with VIP21-caveolin cDNA were pulse-labeled for 7 min and chased for up to 20 min. Cells solubilized at different times of chase were immunoprecipitated and treated as described in panel A, except that the immunoprecipitates were solubilized in the alkaline

The Hydrophobic Segment of VIP21-Caveolin Is a Signal/Anchor, Mediating the Cotranslational Insertion of the Protein into the Microsomal Membranes through the Classical Translocation Machinery

Although VIP21-caveolin was shown to be localized to the TGN, to the TGN-derived vesicles, and to the caveolae, the actual site of integration of VIP21-caveolin into the membranes is not known. In addition, data concerning the orientation of the protein within the membrane are controversial (Dupree *et al.*, 1993; Lisanti *et al.*, 1993; Sargiacomo *et al.*, 1993).

The amino acid sequence of VIP21-caveolin predicts no cleavable aminoterminal signal peptide but shows a single hydrophobic sequence of 33 amino acids located 101 residues after the initial methionine and followed by a 43-residue carboxy tail. We examined whether this hydrophobic stretch could serve as a signal sequence and mediate the insertion of VIP21-caveolin into the ER membrane using the usual membrane/secretory protein pathway. We used an *in vitro* transcription-translation-translocation system, which allowed us to study whether the insertion of VIP21-caveolin into the membrane was

Figure 5. VIP21-caveolin becomes inserted in the membrane cotranslationally, via the classical ER translocation machinery. The *in vitro*-produced VIP21-caveolin RNA was used to program synthesis in the wheat germ extract: (A) in the absence of dog pancreas microsomes (DPM, lanes 1–3, "[minus]"), in the presence of DPM added at the beginning of the translation (lanes 4–6, "co"), or added after the translation was completed (lanes 7 to 9, "post"); (B) in the presence of PKRM added at the beginning of the translation, alone (lanes 1–3), or together with SRP (lanes 4–6); (C) in the presence of reconstituted vesicles



containing docking protein (DP) and TRAM (lanes 1 and 2) or containing these two proteins plus Sec61 (lanes 3 and 4). Two-thirds of the translation mixture was submitted to flotation in the presence of high salt (A) or in alkaline pH (B and C) to separate the membrane fraction (M) containing the integral membrane proteins from the fraction containing the noninserted, free protein (F). The rest of the total mixture (T) before fractionation is also shown in panels A and B. Arrow designates VIP21-caveolin.

cotranslational, SRP dependent, and needed docking protein (SRP receptor) and Sec61.

Dog pancreas microsomes were added at the beginning of translation or after the synthesis was completed. Insertion of VIP21-caveolin into the membrane was estimated by flotation of the translation product in the presence of high salt or of alkaline pH. As shown in Figure 5A, a substantial amount of VIP21-caveolin was found in the membrane fraction (Figure 5A, lane 5) only when membranes were added cotranslationally (Figure 5A, lanes 4–6). In the absence of membrane (Figure 5A, lanes 1–3) or when the membranes were present post-translationally (Figure 5A, lanes 7–9), a very small amount of VIP21-caveolin was associated with the membrane (Figure 5A, lanes 2 and 8).

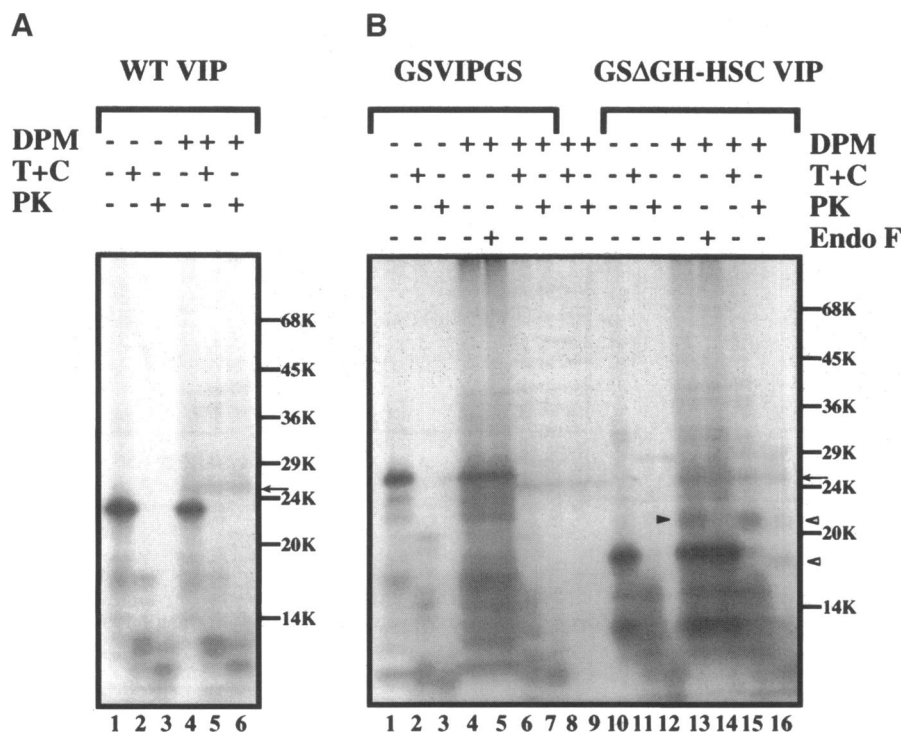
The insertion of VIP21-caveolin was dependent on the presence of SRP in the assay (Figure 5B). The puromycin, potassium washed membranes (PKRM), depleted of SRP, poorly supported the association of VIP21-caveolin with the membranes (lane 2), whereas the addition of exogenous SRP to the same membrane preparation led to a high increase of the VIP21-caveolin found in the membrane fraction (Figure 5B, lane 5 compared with lane 2).

Furthermore, proteoliposomes reconstituted with purified Sec61, docking protein, and TRAM (Görlich and Rapoport, 1993), identified as necessary and sufficient components of the translocation apparatus, were competent for VIP21-caveolin insertion (Figure 5C, lane 3). By contrast, reconstituted proteoliposomes in which Sec61 was omitted were poorly efficient for the VIP21-caveolin insertion (Figure 5C, lane 1).

Taken together, these results show that VIP21-caveolin becomes inserted while it is synthesized by the ER-bound ribosomes, that its insertion is performed by the "classical" membrane/secretory protein translocation machinery, and that consequently the hydrophobic domain serves as a signal/anchor.

Topology of VIP21-Caveolin

The disposition of VIP21-caveolin within the membranes was studied on the *in vitro*-inserted VIP21 by a protease protection assay. Both proteinase K and a mixture of trypsin/chymotrypsin were used. As shown in Figure 6A, the free VIP21-caveolin synthesized in the absence of membrane and the membrane-inserted protein showed a similar digestion pattern when proteases were added to the translation mixture after the synthesis (Figure 6A, compare lanes 2 and 5 and lanes 3 and 6, respectively). This indicates that the insertion of VIP21-caveolin in the membrane did not alter the sensitivity of the protein to protease activity. Because the N-terminal, hydrophobic, and C-terminal segments all contain methionine residues, any translocated and thus protected fragment would have been visible, as is the mature form of a secretory protein (GH) precursor synthesized and processed in the same conditions (Monier *et al.*, 1988). This topology was confirmed by testing a modified VIP21, GSVIPGS, in which two glycosylation sites were added, one at the N-terminus at position 2, the other at the C-terminus at position 179, just before the stop codon. As shown in Figure 6B, this new form of VIP21 did not become glyco-



(lanes 2, 6, 11, and 15) or with proteinase K (lanes 3, 7, 12, and 16) as described in panel A, or with endoglycosidase F (Endo F, lanes 5 and 14). The closed arrowhead points to the glycosylated form of the fusion protein, the open arrowheads to its protected fragments, the arrow to the background band also present when DPM alone was used and treated with the proteases (lanes 8 and 9).

synthesized upon addition of DPM (Figure 6B, compare lanes 1 and 4–5). Again, no protected fragment different from the ones observed in the absence of membrane was detected (Figure 6B, lanes 2–3 and 6–7). The bands marked with an arrow are nonspecific for this construct and are present also when membranes alone, without RNA, were treated in the same conditions (Figure 6B, see lanes 8 and 9).

These results indicate that neither the N- nor the C-terminus of the native VIP21 or of GSVIPGS reached the microsomal lumen. The disposition of VIP21-caveolin within the membrane was therefore in a loop configuration, exposing the bulk of the protein to the cytoplasmic surface of the microsomes.

The formation of the unusual hairpin structure hereby detected was then shown to be dependent on the presence of the amino terminal domain of VIP21-caveolin. The N-portion flanking the hydrophobic region was deleted and replaced by a sequence derived from GH deleted of its signal peptide and including a glycosylation site (see MATERIAL AND METHODS); the hydrophobic domain and the carboxy tail remained unmodified. In contrast to the results just described, a fraction of GSΔGH-HSC VIP became glycosylated upon addition of microsomal membranes (Figure 6B, closed

Figure 6. Both regions flanking VIP21-caveolin hydrophobic segment are located on the cytoplasmic surface of the ER; the replacement of the N-domain of VIP21-caveolin leads to a misorientation of the hydrophobic domain within the membrane. (A) After synthesis in the absence (lanes 1–3) or in the presence of DPM (lanes 4–6), a portion of the translation mixture containing the wild-type VIP21-caveolin (WT VIP) was mock-treated (lanes 1 and 4), or treated with a mixture of trypsin/chymotrypsin at 0.14 mg/ml each for 80 min on ice (T+C, lanes 2 and 5), or treated with 0.7 mg/ml proteinase K for 1 h on ice (PK, lanes 3 and 6). (B) VIP21-caveolin bearing two glycosylation sites (GSVIPGS, lanes 1–7) and a fusion protein, GSΔGH-HSC VIP (lanes 10–16), were synthesized in the absence or in the presence of DPM. GSΔGH-HSC VIP contains only the hydrophobic domain and the C tail of VIP21-caveolin (amino acids 102–178) added downstream from a GSΔGH segment consisting of a glycosylation site (GS) followed by the amino acids 42–130 of rat pre-growth hormone (ΔGH). They were treated post-translationally either with trypsin/chymotrypsin

arrowhead, lane 10 compared with lane 13). The glycosylated protein was sensitive to the endoglycosidase F treatment (Figure 6B, lane 14). Upon treatment with trypsin/chymotrypsin, the fusion protein generated a protected fragment, which comigrated with the glycosylated form of the protein (Figure 6B, lane 15); the other fragments were not specific for the membrane-associated form (Figure 6B, compare lanes 11 and 15). The digestion with proteinase K, which has a broader spectrum than trypsin and chymotrypsin, yielded also to the production of protected peptides specific for the membrane-processed form (Figure 6B, open arrowheads, compare lane 16 with lane 12). This indicates that the N-region of this fusion protein was translocated into the lumen of the vesicles. When the same segment GSΔGH was added upstream to the full length VIP21-caveolin, the new protein GSΔGH-FL VIP did not become glycosylated although it was membrane associated (our unpublished result). This result indicates that the topology of this protein was the same as the one of the wild-type VIP21-caveolin and of GSVIPGS. A fusion protein made of GSΔGH linked to the C-tail of VIP21-caveolin was used as a control and was not membrane inserted and not glycosylated (our unpublished result). This last result confirmed that the hydrophobic segment of

VIP21-caveolin indeed had the function of a signal peptide.

Taken together, these observations show that the presence of the sequence including the hydrophobic stretch plus the C-tail, from residues 102–178, was not sufficient to induce the loop configuration and to prevent the region preceding it to cross the membrane bilayer. This suggests that the stable hairpin structure observed in the native VIP21-caveolin may result from interactions between the regions flanking the signal/anchor.

VIP21-Caveolin Forms Oligomers In Vitro

Because the VIP21-caveolin oligomerization process was shown to be an early post-translational event, possibly taking place in the ER or in a close post-ER compartment, we studied whether oligomerization of in vitro-synthesized VIP21-caveolin could occur. Our previous results showing that oligomers consisted of both isoforms of VIP21-caveolin led us to test them both. It was proposed, according to a mass spectrometry study (Dupree, Kellner, and Kurzchalia, unpublished data), that the smaller isoform of VIP21-caveolin would derive from the longer one by the use of an alternative initiation codon located 32 residues after the first one. The smaller isoform, then named truncated VIP (TR VIP) was therefore generated for the in vitro purposes by deleting the nucleotides encoding the first 31 amino acids of the full length clone, or wild-type VIP (WT VIP). In vitro-synthesized TR VIP indeed comigrated with the small isoform of VIP21-caveolin immunoprecipitated from metabolically labeled MDCK cells. Figure 7 shows that VIP21-caveolin could also, in vitro, be found in high molecular mass complexes. Both TR VIP and WT VIP were able to generate oligomers (Figure 7, panels A and C, respectively), although TR VIP was much more efficient: about 12% of the protein was found in the form of oligomers. TR VIP produced two major species of complexes of about 200 and 400 kDa, of similar sizes as those detected in vivo, and several minor bands of approximately 190, 320, and 600 kDa. They resolved into monomers upon boiling in alkaline SDS-PAGE sample buffer (Figure 7, panel B, compare lanes 6 and 7). The complexes containing the WT VIP were of slightly different size (Figure 7C), about 300 and 600 kDa. The complexes formed, in both cases, only when VIP21-caveolin was inserted into the ER membranes (Figure 7, A and C, compare lanes 1 and 2) and when cytosol was added to the assay (Figure 7B, compare lanes 1 and 6). The amount of complexes formed in vitro increased as a function of the amount of cytosol added in the post-translational assay (Figure 7B, compare lanes 2–6 to lane 1) and as a function of incubation time: after 5 min the oligomers could be detected,

after 1 h, the maximal was reached (our unpublished result).

That the VIP21-caveolin insertion into the membrane was a prerequisite for a cytosol-dependent oligomerization was demonstrated by the fact that no TR VIP oligomer was formed 1) when membrane non-competent for translocation (depleted of SRP) was used, or 2) when membrane was added post-translationally. Furthermore, the amount of complexes formed during the post-translational assay increased as a function of membrane-inserted TR VIP present in the assay. In contrast, free nonlabeled in vitro-produced TR VIP, synthesized in the absence of membrane, added in increasing amount to a fixed quantity of labeled membrane-inserted VIP, did not alter the amount of formed complexes. This rules out the possibility of a nonspecific aggregation of VIP21-caveolin due to some structural feature like, for example, the presence of a long hydrophobic domain sticking to the membrane, a process facilitated or promoted by cytosol. Moreover, the oligomerization studied in vitro was clearly not induced by treatment of the post-translational mixture by the detergent SDS. Indeed, when the post-translational assay was performed at 4°C and then the detergent added to the sample for SDS-PAGE processing, no oligomer was detected (Figure 7A, lane 8). The oligomer formation was blocked by addition of 10 mM GMP-PCP to the cytosol (Figure 7D, lane 2 compared with lane 1), as well as by depletion of the ATP content of cytosol by addition of hexokinase-deoxyglucose (Figure 7D, lane 8 compared with lane 6). Addition of EDTA, but not of EGTA, abolished VIP21-caveolin oligomerization (Figure 7D, lanes 3 and 4, respectively). Such dependence of oligomer formation on GTP- and ATP-hydrolysis, and on the presence of Mg²⁺ but not of Ca²⁺ again rules out the possibility that the oligomers we could generate from in vitro-synthesized VIP were merely the result of SDS action on the protein. The complexes formed in vitro were not CHAPS insoluble and were found in the supernatant phase after the detergent extraction (Figure 7B, lanes 9 and 10), whereas their counterparts purified from tissue or cells were insoluble (see Kurzchalia *et al.*, 1992).

Finally, the sensitivity of the complexes to the trypsin/chymotrypsin (T+C) treatment was studied. The complexes were incubated with the proteases just after the post-translational assay, before any detergent addition, and generated degradation products visible as smears (Figure 7E, lane 9) of about 68, 200, and 300 kDa. Only the 200- and the 68-kDa smears were detected when proteinase K, which has a broader spectrum, was used instead of T+C (our unpublished observation). When the post-translational mix was first complemented with 0.5% Triton X-100, the profile of the complexes obtained was slightly modified (Figure 7E, compare lanes 8 and 10): the complexes higher

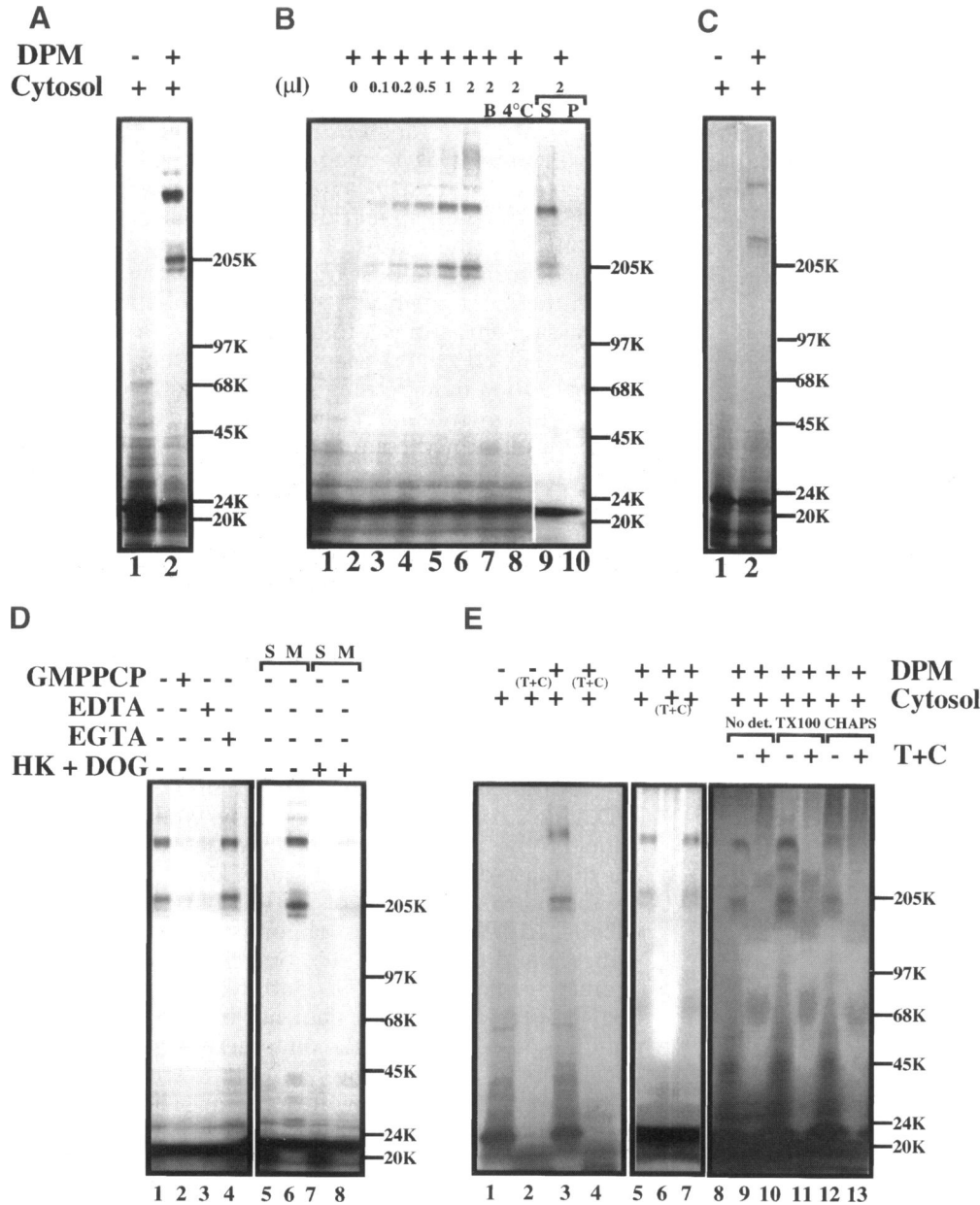


Figure 7. VIP21-caveolin, inserted into the microsomal membranes *in vitro*, oligomerizes in a cytosol-dependent manner. (A and C) After a 90-min translation in the absence (lane 1) or in the presence of DPM (lane 2), 5 μ l of TR VIP (A) or of WT VIP (C) was incubated at 30°C for 1 h in the presence of MDCK cytosol. Samples were then solubilized in the alkaline SDS-PAGE sample buffer and loaded on the 3–16% acrylamide gradient gel without boiling. (B) After synthesis of TR VIP in the presence of DPM, 4 μ l aliquots of translation mixture were centrifuged and resuspended in 4 μ l of HMKD buffer, supplemented with various amounts of MDCK cell cytosol as indicated at the top of the figure (lanes 2–10) or buffer alone (lane 1) and incubated for 60 min at 30°C for all samples except the one in lane 8, which was incubated at 4°C. After the post-translational incubation, samples were treated as described in A and C, except for the sample in lane 7, which was boiled, and one sample that was treated with CHAPS and centrifuged; the supernatant (S, lane 9) and the pellet (P, lane 10) were treated as described for A and C. (D) TR VIP translated in the presence of DPM was incubated in the presence of cytosol alone (lane 1), in the presence of cytosol supplemented with 10 mM GMP-PCP (lane 2), 10 mM EDTA (lane 3), or 10 mM EGTA (lane 4) for 1 h at 30°C. In lanes 5–8, identical aliquots of the translation were used, but were centrifuged before the post-translational assay and separated into the membrane

pellet (M, lanes 6 and 9) and supernatant (S, lanes 5 and 7). Cytosol alone (lanes 5 and 6) or cytosol plus deoxyglucose (DOG) and hexokinase (HK) (lanes 7 and 8) was added and incubated as described above. Samples were processed as in A and C. (E) TR VIP was synthesized in the presence or in the absence of DPM and, in the post-translational assay, in the presence or in the absence of cytosol, as indicated on the figure. The digestion with trypsin/chymotrypsin (T+C) for 80 min on ice followed by the inactivation of the enzymes by a protease inhibitor was performed either on the translation products before addition of cytosol (lanes 2 and 4), or on the cytosol before its addition to the translation mix (lane 6), or on the samples after incubation with cytosol (lanes 9, 11, and 13). The samples described in lanes 8 to 13 were either not treated with detergent (no det, lanes 8 and 9), complemented with 0.5% Triton X-100 (TX100, lanes 10 and 11), or extracted with 20 mM CHAPS (lanes 12 and 13) before the protease treatment; in the former case, the supernatant fraction contained the oligomers (see Figure 7B, lane 9) and is shown in lanes 12 and 13. The sample in lane 7 was incubated in the presence of cytosol plus the protease inhibitor alone. Samples were processed as in panels A and C.

than 400 kDa disappeared while a minor species (the product of approximately 300 kDa) became more prominent. The addition of T+C to the Triton X-100–

treated complexes (Figure 7E, lane 11) or to the complexes found in the supernatant fraction after CHAPS extraction (Figure 7E, lane 13), yielded to the appear-

ance of degradation products of similar size to the ones obtained in the absence of detergent (Figure 7E, lane 9), except for the 300-kDa product, which was not present when the CHAPS fraction was digested. These data indicate that the presence of Triton X-100 and CHAPS, and consequently the modification of the lipid environment of the oligomers, did not alter the overall structure of the complexes because no additional recognition sites for the proteases was revealed, as compared with the samples not treated with detergent. However, there were minor changes in the properties of the complexes: the very large forms of the complexes (more than 600 kDa) seemed to be better solubilized by Triton X-100, and CHAPS made TR VIP in the 300-kDa complex more accessible to proteases. As controls, the VIP-containing microsomes and the cytosol were independently treated with proteases before their use in the post-translational assay. This treatment led to the partial degradation of TR VIP (Figure 7E, lanes 2 and 4) and abolished its capacity to oligomerize in the presence of cytosol (Figure 7E, lane 4 compared with lane 3). Similarly, a T+C-treated cytosol failed to induce the oligomerization of TR VIP (Figure 7E, lane 6). It must be noted that the protease inhibitor used for inactivating the enzymes had no influence on the complex formation (Figure 7E, lane 7) and totally inhibited the protease activity as observed in Figure 7E, lane 6, where the amount of the monomeric form of TR VIP was the same as when no protease was used (Figure 7E, compare lane 6 with lane 5).

The Oligomerization of the In Vitro Membrane-inserted VIP21-Caveolin Does Not Involve a Vesicle Fusion Step

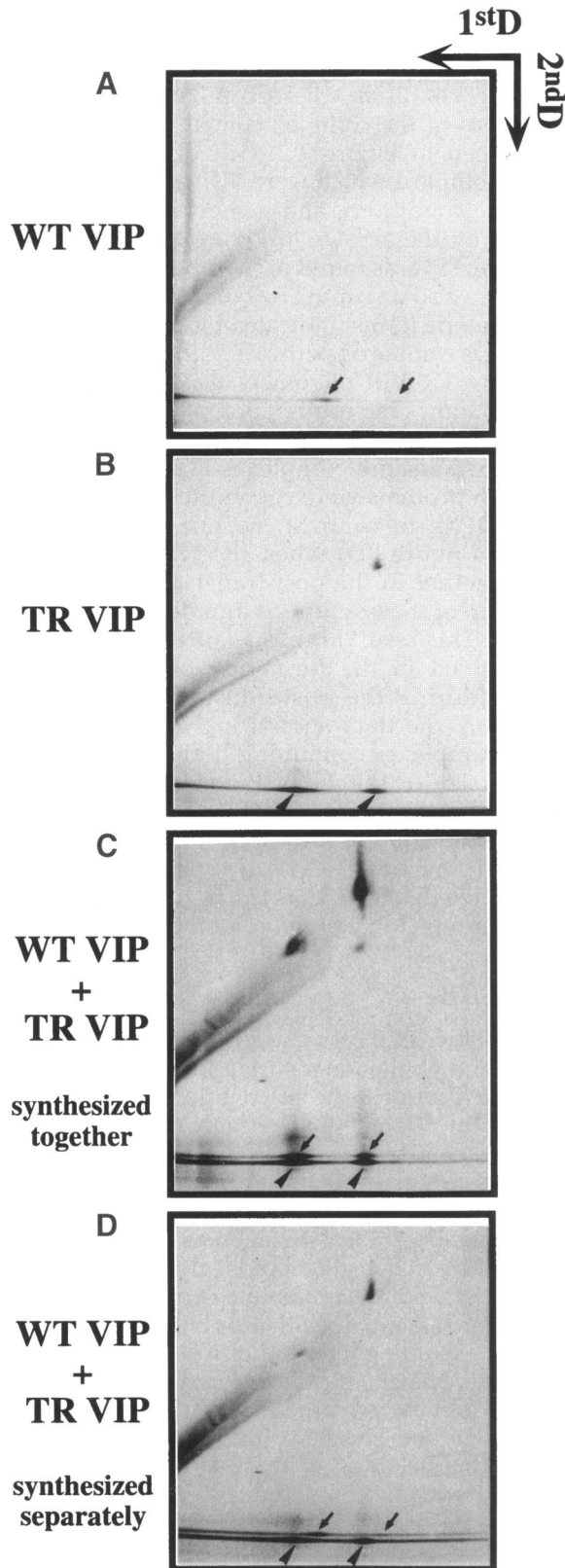
The formation of high molecular mass complex from monomers implies the accumulation of the protein within membrane microdomain, which would make it possible for the protein monomers to oligomerize under the control of a cytosolic factor(s); indeed, at least 15 molecules of VIP21-caveolin should theoretically be present in a single vesicle to form a 400-kDa complex. This could be the result of a VIP21-caveolin clustering in a particular region of the membrane, or, alternatively, this could be achieved by the fusion of several vesicles, each one possibly having a low content of inserted VIP21-caveolin.

We tested whether the oligomer formation involved a step of vesicle fusion by generating three different populations of microsomes in vitro: one containing the membrane-inserted WT VIP, one the TR VIP, and one in which both the WT and the TR VIP were cotranslationally inserted. The post-translational assay was then performed on the three types of vesicles and in a fourth test tube in which an equivalent amount of membrane-inserted TR and WT VIP was added. The

reaction products were analyzed on 2D gel, as described in MATERIAL AND METHODS: the first dimension allows the separation of the complexes under nonboiling condition, the second dimension allows the analysis of the complex content after boiling. As already seen in Figure 7C, WT VIP generated two types of complex, which were disrupted upon boiling in alkaline conditions, and generated the monomers indicated by the arrows in Figure 8A. Similarly, TR VIP (Figure 8B) was found in two species of oligomers, which were also disrupted by boiling; the migration of the monomeric forms (indicated by arrowheads) more to the left as compared with WT VIP, indicates that the size of the TR VIP oligomers was slightly smaller. Figure 8C shows the comigration of both WT VIP and TR VIP monomers, indicating that both isoforms were present in the same complexes. This was achieved when both proteins were co-synthesized in the presence of DPM. In contrast, no mixed complex was observed (Figure 8D) when the two proteins were added together in the post-translational assay after completion of their synthesis and of their membrane insertion. This result argues against a vesicle fusion step involved in the formation of VIP21-caveolin oligomer during the post-translational incubation. In addition, the data shown in Figure 8C indicate that the complexes containing both WT and TR VIP were the size of the TR VIP-generated complexes, and not the size of the WT VIP-generated complexes. This latter observation together with the higher efficiency of TR VIP to form complexes may be indicative that TR VIP is the initiator, and may be a nucleation factor, for the oligomer formation.

DISCUSSION

Our present work shows that VIP21-caveolin, found in the TGN and on the inner surface of the plasma membrane as a part of the coat covering the caveolae, is able to form oligomers. The high molecular weight structures seem to be composed for the major part of VIP21-caveolin and membranes; indeed, the complex insolubility in detergents such as CHAPS and Triton, and its flotation ability are taken as lines of evidence for a structure rich in glycolipids (glycosphingolipids). The VIP21-caveolin-containing complexes could be resolved into essentially either or both VIP21-caveolin isoforms, excluding any other products. This was shown for the biochemically isolated 400-kDa complex as well as for newly synthesized VIP21-caveolin polymers in vivo and for the complexes formed in vitro. Previous reports showing that VIP21-caveolin can be co-isolated with various other cell components sharing the same biological properties, for example the Triton X-100 insolubility of VIP21-caveolin, GPI-anchored proteins, glycosphingolipids, and others (Fiedler *et al.*, 1993; Lisanti *et al.*, 1994), have correlated this



with a physiologically relevant protein-protein interaction. However, our results strongly suggest that VIP21-caveolin has the primary capacity of oligomerizing and that the high molecular mass complexes represent the forms under which VIP21-caveolin is found in the detergent-insoluble fraction. Whether these structures, visualized as ovoid after a mild SDS treatment, may represent the basic unit of the striated coat covering the inner surface of caveolae (Rothberg *et al.*, 1992), and whether VIP21-caveolin already assembled in oligomers in the ER is still compatible with its possible role in the sorting of caveolae-destined proteins (Sargiacomo *et al.*, 1993), remain to be clarified.

Unlike other coat proteins identified so far, VIP21-caveolin is an integral membrane protein, and, as shown in this paper, it becomes integrated into the membrane in the ER, where it is synthesized. Its unique hydrophobic domain, which then must serve as a signal peptide and as a signal anchor, is located 101 amino acids after the initial methionine and is followed by a short C tail (43 residues), and must emerge from the synthesizing ribosomes nearly at the same time as the peptide chain terminates. However the integration of the protein within the membrane is clearly cotranslational and involves the now well defined components for ER translocation, SRP and the docking protein on the one hand, and Sec61 and TRAM making the translocation machinery itself on the other hand. This process confers VIP21-caveolin the following and unusual topology: the hydrophobic domain is anchored in the membrane in a loop configuration exposing both its N- and C-flanking regions to the cytoplasmic surface of the microsomes, as already suggested by immunofluorescence studies (Dupree *et al.*, 1993). The hairpin structure could be altered by changing the whole N-region located upstream from the anchor of VIP by a sequence of a similar size deriving from the GH sequence: this fusion protein, GSΔGH-HSCVIP, adopted the type I membrane protein orientation. This indicates that the hydrophobic domain and the C terminal tail of the protein are not sufficient to confer VIP21-caveolin the correct orienta-

Figure 8. The post-translational formation of VIP21-caveolin complex does not involve a vesicle fusion step. WT and TR VIP were synthesized separately or together in the presence of DPM. In the post-translational assay the following conditions were included: WT VIP alone (A), TR VIP alone (B), WT and TR VIP synthesized together (C), and WT VIP plus TR VIP, previously synthesized separately in the presence of DPM (D). All four samples were incubated in the presence of HeLa cytosol. The reaction products were solubilized at room temperature in the standard SDS-PAGE sample buffer, and analyzed in the first dimension on a 2.5–7.5% acrylamide gradient gel. Each lane was cut, boiled in alkaline SDS-PAGE sample buffer, and analyzed in the second dimension on a 3–16% acrylamide gradient gel. The arrows indicate the WT VIP, the arrowheads indicate the TR VIP.

tion and suggests that some structural feature present in the N domain of the protein is necessary for the hydrophobic domain to form the loop by which the native VIP21-caveolin becomes inserted into the membrane. However, our results do not exclude the possibility that VIP21-caveolin does not cross the entire membrane bilayer but is a monotopic membrane protein (according to the classification of Blobel, 1980), as recently demonstrated for the integral membrane protein, the prostaglandin H₂ synthase-1 (Picot *et al.*, 1994).

The complex formation shows a complete dependence on the presence of membrane-inserted VIP21-caveolin. No complex could ever be observed when free VIP21-caveolin, VIP21-caveolin synthesized in the presence of translocation incompetent membrane (membrane deleted of SRP), or VIP21-caveolin synthesized before addition of membrane, was used in the post-translational assay. The proper membrane disposition of VIP21-caveolin is an essential but not sufficient requirement for the complex formation. Indeed no complex could be formed by the fusion protein GSΔGH-HSC VIP exposing only the C tail of VIP to the cytoplasmic surface of the membrane. GSΔGH-FL VIP, which adopts the same topology as the WT VIP, was not able to generate oligomers in the tested conditions (our unpublished result). Our data also indicate that the first 31 amino acids of the protein have a strong inhibitory effect on the complex formation, as shown for the WT VIP low efficiency to form the oligomers as compared with the TR VIP tested in the same conditions. The inhibitory role of the N-extremity might be even exacerbated when an extra amino acid sequence is added upstream from it, as suggested by the inability of GSΔGH-FL VIP to make complexes. Moreover, deleted N-terminal sequences consisting of amino acids 32–80 on the one hand or residues 80–101 on the other hand, linked to the rest of the protein, were not sufficient to induce VIP21-caveolin oligomerization (our unpublished observations).

The active sequence, including at least a sequence comprised between amino acids 32 and 101, is under the control of a cytosolic factor(s) present in two mammalian cell lines but not in the plant cytosol, and which would be involved in mobilizing together the VIP21-caveolin protein already present in the bilayer. About 7, 15, or 22 molecules would be found in the various complexes and modified in such a way that SDS at room temperature has no access to critical sites leading to the disruption of these structures. It is important to note that the *in vitro*-generated complexes are not CHAPS insoluble, which is in good agreement with the fact that insolubility may be linked to the presence of glycosphingolipids, known to be synthesized in early Golgi. Very little, if any, Golgi-derived vesicles are present in the dog pancreas microsomes prepared for the *in vitro* translocation. This observa-

tion suggests that the complex formation and the acquirement of detergent insolubility are, in the case of VIP21-caveolin, not simultaneous events.

We propose that the complex formation is a very early post-translational process, which takes place in the ER and does not seem to involve vesicle fusion, but rather the clustering of membrane-inserted VIP21-caveolin. The detergent insolubility may be linked to the passage of VIP21-caveolin complex through the Golgi cisternae or the TGN, where the carrier vesicles will acquire the detergent insoluble glycosphingolipids (Brown and Rose, 1992; van Meer, 1993, for a review). However, to date, we have no evidence that VIP21-caveolin complexes transit through the Golgi apparatus to the plasma membrane. The complexes might also acquire their detergent insolubility as they reach the plasma membrane, directly without passing through the TGN, by the same carrier vesicles that may be responsible for the transport of cholesterol from the ER to the cell membrane (Urbani and Simoni, 1990). The complexes could subsequently be found in the TGN after internalization of the caveolae as recently described by Parton *et al.* (1994), or of the caveolin itself as suggested by Smart *et al.* (1994). This possibility is, however, not likely because a high content of cholesterol should confer the CHAPS insolubility to the VIP21-caveolin-containing vesicles obtained *in vitro*.

Recently published reports have proposed that the formation of detergent-insoluble oligomers would be correlated with their retention in the compartment where this step occurs (Weisz *et al.*, 1993; Schweizer *et al.*, 1994). The VIP21-caveolin complex we are able to detect *in vitro* may correspond to an intermediate step of the mature, steady-state detergent-insoluble VIP21-caveolin complex. The possibility to define two steps, oligomerization and insolubility, may allow us to better dissect the processes underlying a membrane protein processing. Such a multistep process has been well analyzed for a secretory protein, the von Willibrand factor (Voorberg *et al.*, 1993), which forms disulfide bond-linked dimers in the ER; further processing occurs in the Golgi apparatus where it is found in the form of high molecular weight multimer. Similarly, trimerization of influenza virus hemagglutinin is a late ER event necessary for the protein exit from the ER, and does not lead to detergent insolubility, which takes place in the late Golgi. Unlike VIP21-caveolin complex formation, oligomerization or subunit assembly so far characterized involves disulfide bond formation (Braakman *et al.*, 1992), which is an intraluminal reaction probably independent of cytosolic factors. The assembly processes have been shown to be, at least partly, under the control of chaperones, which by an early interaction with either the nascent chain or the just terminated protein, would prevent the misfolding of the protein (see Gething and Sambrook,

1992), and/or would help in maintaining the proper disposition which will then be recognized by other molecules catalyzing proper folding, maturation of a propeptide, or interaction with other subunits. This has been shown, for example, for the ER lumen BiP and the processing of thyroglobulin (Kim *et al.*, 1992), the 7B2 neuroendocrine chaperone involved in the secretory pathway (Braks and Martens, 1994), the cytosolic chaperones of the hsp 70 family and their interaction with newly synthesized proteins (Pelham, 1989; Beckmann *et al.*, 1990). A similar process is also likely to be involved during VIP21-caveolin biosynthesis of the long N terminus, waiting until the rest of the molecule is available for the SRP interaction and subsequent membrane incorporation. The formation of the high molecular weight complexes later made by the completed VIP21-caveolin is also likely to be under the control of a chaperone(s) provided by the cytosol. However, this oligomerization process probably is of a different nature than the early post-translational reactions just described for the following reasons: 1) the complexes detected *in vitro* are of the same size as the "mature" ones detected *in vivo*; 2) they do not involve disulfide bonds; 3) their formation is not only ATP hydrolysis and Mg^{2+} dependent, but also GTP hydrolysis dependent. In contrast to the oligomerization in the ER of rotavirus proteins (Poruchynsky *et al.*, 1991), VIP21-caveolin complex formation is calcium independent. In addition, the complexes form exclusively from the native VIP21-caveolin and from the smaller isoform lacking the first 31 residues. All these observations render it very unlikely that VIP21-caveolin oligomers represent the multimolecular complexes or aggregates observed in the ER, made of terminally misfolded proteins, and on the way to an active conformation or to accelerated proteolysis. It is noteworthy that a member of the hsp70 family, the uncoating enzyme, hydrolyses ATP in a clathrin-dependent manner, driving disassembly of the clathrin coat (Ungewickell, 1985). A similar assembly/disassembly of the caveolar coat may also occur under the control of a specific cytosolic chaperone(s) interacting either with the caveolar coat to disassemble it or with the membrane-inserted VIP21-caveolin to promote assembly. Identification of the factor(s) involved in oligomerization should give important information about the mechanism of the caveolar coat formation.

ACKNOWLEDGMENTS

We thank Dr. Paul Dupree (University of Cambridge, UK) for the generous gift of VIP21 antibody and Dr. Bill Dolan (NYU Medical Center, New York, NY) for HeLa cells. We are indebted to Berit Jungnickel and Dr. Tom Rapoport (MDC, Berlin-Buch) for SRP and reconstituted proteoliposomes, and to Dr. Hans Böhm for sequencing VIP21-caveolin constructs. Dr. Paul Dupree, Ulrike Kutay, and Dr. Tom Rapoport are also thanked for conceptual discussions and

the critical reading of the manuscript. This work was supported in part by a grant from the Deutsche Forschungsgemeinschaft to T.V.K.

REFERENCES

- Anderson, R.G.W. (1991). Molecular motors that shape endocytic membrane. In: *Intracellular Trafficking of Proteins*. ed. C.J. Steer and J.A. Hanover, London, UK: Cambridge University Press, 13–16.
- Anderson, R.G.W. (1993a). Plasmalemmal caveolae and GPI-anchored membrane proteins. *Curr. Opin. Cell Biol.* 5, 647–652.
- Anderson, R.G.W. (1993b). Caveolae: where incoming and outgoing messengers meet. *Proc. Natl. Acad. Sci. USA* 90, 10909–10913.
- Anderson, R.G.W., Kamen, B.A., Rothberg, K.G., and Lacey, S.W. (1992). Potocytosis: sequestration and transport of small molecules by caveolae. *Science* 255, 410–411.
- Arreaza, G., Melkonian, K.A., LaFevre-Berut, M., and Brown, D.A. (1994). Triton X-100-resistant membrane complexes from cultured kidney epithelial cells contain the src family protein tyrosine kinase p62^{es}. *J. Biol. Chem.* 269, 19123–19127.
- Beckman, R.P., Mizzen, L.A., and Welch, W.J. (1990). Interaction of Hsp70 with newly synthesized proteins: implications for protein folding and assembly. *Science* 248, 850–854.
- Behlke, J., Bommer, U.-A., Lutsch, G., Henske, A., and Bielka, H. (1986). Structure of initiation factor eIF-3 from rat liver: hydrodynamic and electron microscopic investigations. *Eur. J. Biochem.* 157, 523–530.
- Blobel, G. (1980). Intracellular protein topogenesis. *Proc. Natl. Acad. Sci. USA* 77, 1496–1500.
- Braakman, I., Helenius, J., and Helenius, A. (1992). Manipulating disulfide bond formation and protein folding in the endoplasmic reticulum. *EMBO J.* 11, 1717–1722.
- Braks, J.A.M., and Martens, G.J.M. (1994). 7B2 is a neuroendocrine chaperone that transiently interacts with prohormone convertase PC2 in the secretory pathway. *Cell* 78, 263–273.
- Brown, D.A., and Rose, J. (1992). Sorting of GPI-anchored proteins to glycolipid-enriched membrane subdomains during transport to the apical cell surface. *Cell* 68, 533–544.
- Chang, W.-J., Ying, Y.-S., Rothberg, K.G., Hooper, N.M., Turner, A.J., Gambliel, H.A., de Gunzburg, J., Mumby, S.M., Gilman, A.G., and Anderson, R.G.W. (1994). Purification and characterization of smooth muscle cell caveolae. *J. Cell Biol.* 126, 127–138.
- Compton, T., Ivanov, I.E., Gottlieb, T., Rindler, M., Adesnik, M., and Sabatini, D.D. (1989). A sorting signal for the basolateral delivery of the vesicular stomatitis virus (VSV) G protein lies in its luminal domain: analysis of the targeting of VSV G-influenza hemagglutinin chimeras. *Proc. Natl. Acad. Sci. USA* 86, 4112–4116.
- Dupree, P., Parton, R.G., Raposo, G., Kurzchalia, T.V., and Simons, K. (1993). Caveolae and sorting in the *trans*-Golgi network of epithelial cells. *EMBO J.* 12, 1597–1604.
- Fiedler, K., Kobayashi, T., Kurzchalia, T.V., and Simons, K. (1993). Glycosphingolipid-enriched detergent-insoluble complexes are implicated in protein sorting in epithelial cells. *Biochemistry* 32, 6365–6373.
- Fujimoto, T. (1993). Calcium pump of the plasma membrane is localized in caveolae. *J. Cell Biol.* 120, 1147–1157.
- Fujimoto, T., Nakade, S., Miyawaki, A., Mikoshiba, K., and Ogawa, K. (1993). Localization of inositol 1,4,5-trisphosphate receptor-like protein in plasmalemmal vesicles. *J. Cell Biol.* 119, 1507–1514.
- Gething, M.J., and Sambrook, J. (1992). Protein folding in the cell. *Nature* 355, 33–45.

- Ghitescu, L., Fixman, A., Simionescu, M., and Simionescu, N. (1986). Specific binding sites for albumin restricted to plasmalemmal vesicles of continuous capillary endothelium: receptor-mediated transcytosis. *J. Cell Biol.* 102, 1304–1311.
- Glenney, J.R. (1989). Tyrosine phosphorylation of a 22-kDa protein is correlated with transformation by rous sarcoma virus. *J. Biol. Chem.* 264, 20163–20166.
- Glenney, J.R. (1992). The sequence of human caveolin reveals identity with VIP21, a component of transport vesicles. *FEBS Lett.* 314, 45–48.
- Glenney, J.R., and Soppet, D. (1992). Sequence and expression of caveolin, a protein component of caveolae plasma membrane domains phosphorylated on tyrosine in Rous sarcoma virus-transformed fibroblasts. *Proc. Natl. Acad. Sci. USA* 89, 10517–10521.
- Glenney, J.R., and Zokas, L. (1989). Novel tyrosine kinase substrates from Rous sarcoma virus-transformed cells are present in the membrane cytoskeleton. *J. Cell Biol.* 108, 2410–2408.
- Görlich, D., and Rapoport, T.A. (1993). Protein translocation into proteoliposomes reconstituted from purified components of the endoplasmic reticulum membrane. *Cell* 75, 615–630.
- Hoessli, D., and Rungger-Brändle, E. (1985). Association of specific cell-surface glycoproteins with a Triton X-100-resistant complex of plasma membrane proteins isolated from T-lymphoma cells (P1798). *Exp. Cell Res.* 156, 239–250.
- Ivessa, N.E., DeLemos-Chiarandini, C., Tsao, Y.S., Takatsuki, A., Adesnik, M., Sabatini, D.D., and Kreibich, G. (1992). O-Glycosylation of intact and truncated ribophorins in brefeldin A-treated cells: newly synthesized intact ribophorins are only transiently accessible to the relocated glycosyltransferases. *J. Cell Biol.* 17, 949–958.
- Kim, P.S., Bole, D., and Arvan, P. (1992). Transient aggregation of nascent thyroglobulin in the endoplasmic reticulum: relationship to the molecular chaperone, BiP. *J. Cell Biol.* 118, 541–549.
- Kurzchalia, T.V., Dupree, P., Parton, R.G., Kellner, R., Virta, H., Lehnert, M., and Simons, K. (1992). VIP21, a 21-KD membrane protein is an integral component of *trans*-Golgi network-derived transport vesicles. *J. Cell Biol.* 118, 1003–1014.
- Lisanti, M.P., Scherer, P.E., Tang, Z., and Sargiacomo, M. (1994a). Caveolae, caveolin and caveolin-rich membrane rich domains: a signalling hypothesis. *Trends Cell Biol.* 4, 231–235.
- Lisanti, M.P., Scherer, P.E., Vidugiriene, J., Tang, Z., Hermanowski-Vosatka, A., Tu, Y.-H., Cook, R.F., and Sargiacomo, M. (1994b). Characterization of caveolin-rich membrane domains isolated from an endothelial-rich source: implications for human disease. *J. Cell Biol.* 126, 111–126.
- Lisanti, M.P., Tang, Z., and Sargiacomo, M. (1993). Caveolin forms a hetero-oligomeric protein complex that interacts with an apical GPI-linked protein: implications for the biogenesis of caveolae. *J. Cell Biol.* 123, 595–604.
- Monier, S., Van Luc, P., Kreibich, G., Sabatini, D.D., and Adesnik, M. (1988). Signals for the incorporation and orientation of cytochrome P450 in the endoplasmic reticulum membrane. *J. Cell Biol.* 107, 457–470.
- Montesano, R., Roth, J., Robert, A., and Orci, L. (1982). Non-coated membrane invaginations are involved in binding and internalisation of cholera and tetanus toxins. *Nature* 296, 651–653.
- Parton, R.G. (1994). Ultrastructural localization of gangliosides; GM1 is concentrated in caveolae. *J. Histochem. Cytochem.* 42, 155–166.
- Parton, R.G., Joggerst, B., and Simons, K. (1994). Regulated internalization of caveolae. *J. Cell Biol.* 127, 1199–1215.
- Pelham, H.R. (1989). Control of protein exit from the endoplasmic reticulum. *Annu. Rev. Cell Biol.* 5, 1–23.
- Peters, K.-R., Carley, W.W., and Palade, G.E. (1985). Endothelial plasmalemmal vesicles have a characteristic striped bipolar surface structure. *J. Cell Biol.* 101, 2233–2238.
- Picot, D., Loll, P.J., and Garavito, R.M. (1994). The X-ray crystal structure of the membrane protein prostaglandin H₂ synthase-1. *Nature* 367, 243–249.
- Poruchynsky, M.S., Maas, D.R., and Atkinson, P.H. (1991). Calcium depletion blocks the maturation of rotavirus by altering the oligomerization of virus-encoded proteins in the ER. *J. Cell Biol.* 114, 651–656.
- Rothberg, K.G., Heuser, J.E., Donzell, W.C., Ying, Y.-S., Glenney, J.R., and Anderson, R.G.W. (1992). Caveolin, a protein component of caveolae membrane coats. *Cell* 68, 673–682.
- Rothberg, K.G., Ying, Y.-S., Kolhouse, J.F., Kamen, B.A., and Anderson, R.G.W. (1990). The glycopospholipid-linked folate receptor internalizes folate without entering the clathrin-coated pit endocytic pathway. *J. Cell Biol.* 110, 637–649.
- Sargiacomo, B., Sudol, M., Tang, Z., and Lisanti, M. (1993). Signal transducing molecules and glycosyl-phosphatidylinositol-linked proteins form a caveolin-rich insoluble complex in MDCK cells. *J. Cell Biol.* 122, 789–807.
- Schweizer, A., Rohrer, J., Hauri, H.P., and Kornfeld, S. (1994). Retention of p53 in an ER-Golgi intermediate compartment depends on the presence of all three of its domains and on its ability to form oligomers. *J. Cell Biol.* 126, 25–39.
- Simionescu, M., Simionescu, N., and Palade, G.E. (1982). Differentiated microdomains on the luminal surface of capillary endothelium: distribution of the lectin receptors. *J. Cell Biol.* 94, 406–413.
- Smart, E.J., Ying, Y.-S., Conrad, P.A., and Anderson, R.G.W. (1994). Caveolin moves from caveolae to the Golgi apparatus in response to cholesterol oxidation. *J. Cell Biol.* 127, 1185–1197.
- Steer, C.J., and Heuser, J. (1991). Clathrin and coated vesicles: critical determinants of intracellular trafficking. In: *Intracellular Trafficking of Proteins*. ed. C.J. Steer and J.A. Hanover, London, UK: Cambridge University Press, 47–102.
- Tran, D., Carpentier, J.-L., Sawano, F., Gorden, P., and Orci, L. (1987). Ligands internalized through coated or non-coated invaginations follow a common intracellular pathway. *Proc. Natl. Acad. Sci. USA* 84, 7957–7961.
- Ungewickell, E. (1985). The 70-kd mammalian heat shock proteins are structurally and functionally related to the uncoating protein that releases clathrin triskelia from coated vesicles. *EMBO J.* 4, 3385–3391.
- Urbani, L., and Simoni, R.D. (1990). Cholesterol and vesicular stomatitis virus G protein take separate routes from the endoplasmic reticulum to the plasma membrane. *J. Biol. Chem.* 265, 1919–1923.
- Van Meer, G. (1993). Transport and sorting of membrane lipids. *Curr. Opin. Cell Biol.* 5, 661–673.
- Voorberg, J., Fontijn, R., Calafat, J., Janssen, H., van Mourik, J.A., and Pannekoek, H. (1993). Biogenesis of von Willebrand factor-containing organelles in heterologous transfected CV-1 cells. *EMBO J.* 12, 749–758.
- Weisz, O.A., Swift, A.M., and Machamer, C.E. (1993). Oligomerization of a membrane protein correlates with its retention in the Golgi apparatus. *J. Cell Biol.* 122, 1185–1196.